Nodular fasciitis: a novel model of transient neoplasia induced by *MYH9-USP6* gene fusion

Michele R Erickson-Johnson[1,*], Margaret M Chou[2,*], Barbara R Evers[1], Christopher W Roth[1], Amber R Seys[1], Long Jin[1], Ying Ye[2], Alan W Lau[2], Xiaoke Wang[1] and Andre M Oliveira[1]

Nodular fasciitis (NF) is a relatively common mass-forming and self-limited subcutaneous pseudosarcomatous myofibroblastic proliferation of unknown pathogenesis. Due to its rapid growth and high mitotic activity, NF is often misdiagnosed as a sarcoma. While studying the *USP6* biology in aneurysmal bone cyst and other mesenchymal tumors, we identified high expression levels of *USP6* mRNA in two examples of NF. This finding led us to further examine the mechanisms underlying *USP6* overexpression in these lesions. Upon subsequent investigation, genomic rearrangements of the *USP6* locus were found in 92% (44 of 48) of NF. Rapid amplification of 5′-cDNA ends identified *MYH9* as the translocation partner. RT-PCR and direct sequencing revealed the fusion of the *MYH9* promoter region to the entire coding region of *USP6*. Control tumors and tissues were negative for this fusion. Xenografts of cells overexpressing *USP6* in nude mice exhibited clinical and histological features similar to human NF. The identification of a sensitive and specific abnormality in NF holds the potential to be used diagnostically. Considering the self-limited nature of the lesion, NF may represent a model of 'transient neoplasia', as it is, to our knowledge, the first example of a self-limited human disease characterized by a recurrent somatic gene fusion event.

Nodular fasciitis (NF) is a mesenchymal lesion that commonly occurs in the upper extremities, trunk, head and neck of children and young adults.[1,2] The most common clinical presentation is a 2–3-week history of a rapidly growing subcutaneous mass, which is concerning for a possible malignant neoplasm.[1–3] However, NF regresses spontaneously when not surgically resected; thus, it has been clinically viewed as a peculiar reactive process.[1,2] Histologically, NF closely simulates sarcomas because of its high cellularity and high mitotic activity.[1–3] This deceptive histological appearance may result in erroneous diagnoses and inadequate treatment.[4–6]

Since its initial description by Konwaler *et al*,[7] the neoplastic nature of NF has been debated.[8–11] Although a few studies showed evidence that at least a subset of NF were clonal in nature, others were unable to confirm these findings.[8–11] In a few reports where cytogenetical analysis was possible, no specific or consistent recurrent abnormality has been found.[8–11]

We recently identified the *USP6* locus as a recurrent target in aneurysmal bone cyst (ABC), a bone tumor that predominantly occurs in the pediatric population.[12–17] This prompted us to study the biology and possible oncogenic role of *USP6* in other mesenchymal entities. Herein, we report that *USP6* rearrangements with the formation of the fusion gene *MYH9-USP6* occur in most examples of NF. Our finding not only confirms the clonal neoplastic nature of NF, but also suggests a novel model of 'transient neoplasia', as it is, to our knowledge, the first example of a self-limited human lesion characterized by a recurrent somatic gene fusion event.

MATERIALS AND METHODS
Primary Tumors and Controls
Institutional Review Board permission was obtained for this study. Forty-eight cases of NF were identified at Mayo Clinic, Rochester. All cases showed classic histological features: a subcutaneous cellular spindle cell proliferation exhibiting

[1]Department of Laboratory Medicine and Pathology, Mayo Clinic, Rochester, MN, USA; [2]Department of Pathology and Laboratory Medicine, Children's Hospital of Philadelphia, University of Pennsylvania School of Medicine, Philadelphia, PA, USA
Correspondence: Dr AM Oliveira, Department of Laboratory Medicine and Pathology, Mayo Clinic, Rochester, MN 55905, USA.
E-mail: oliveira.andre@mayo.edu
 *These authors contributed equally to this work.

prominent mitotic activity, occasional microcystic changes and extravasated erythrocytes and inflammatory cells.[1,2] Negative controls included four dermatofibrosarcoma protuberans, four myofibromas, three schwannomas, three desmoid-type fibromatoses, three myxofibrosarcomas, three proliferative fasciitis, two proliferative myositis, two neurofibromas, two osteosarcomas, two benign fibrous histiocytomas, two adenocarcinomas, two desmoplastic fibroblastomas, and one each of visceral fasciitis, ischemic fasciitis, giant cell tumor of soft tissues, normal fibroadipose tissue, high-grade undifferentiated pleomorphic sarcoma, leiomyoma, intramuscular myxoma, soft tissue perineurioma, papillary thyroid carcinoma, non-ossifying fibromyxoid tumor of soft parts and capillary hemangioma ($n = 43$). Five ABCs with confirmed *USP6* fusion genes were used as positive controls.

Nucleic Acid Extraction

Frozen tissue was available from two examples of NF. An additional 46 cases of NF were obtained from paraffin blocks or available unstained slides. RNA from frozen samples was mechanically homogenized using Trizol (Invitrogen, Carlsbad, CA) and extracted according to established methods.[18] RNA from formalin-fixed paraffin-embedded (FFPE) samples was extracted using 10-μm sections and by using established methods.[18]

qRT-PCR for USP6

To confirm expression of *USP6* mRNA in NF, qRT-PCR was performed using the LightCycler5 480 Probes Master kit per manufacturer's instruction (Roche, Mannheim, Germany). Quantification was based on the relative expression of target gene (*USP6*) versus a reference gene (*PGK*). All samples were normalized against uterus mRNA. Using Roche's universal primer library (UPL), primers for *USP6* (5′-CCCCCATT ATGATTTTTGAACGG-3′, 5′-TTGTTGTGAACCTCTCCGC AG-3′) and UPL probe 62 (5′-ACCTGCTG-3′), along with primers for *PGK* (5′-GGAGAACCTCCGCTTTCAT-3′, 5′-GC TGGCTCGGCTTTAACC-3′) and UPL probe 69 (5′-GGAGG AAG-3′), were subjected to qRT-PCR using the two index cases of NF, along with two other NFs, two Ewing sarcomas, one synovial sarcoma and three normal tissues (ovary, uterus and myometrium). Testis mRNA was used as a positive control, as *USP6* is primarily expressed in this tissue. Cycling conditions were 94 °C for 10 min, followed by 40 cycles of 94 °C for 10 s, 58 °C for 40 s and 72 °C for 10 s.

Fluorescence *In Situ* Hybridization

Bacterial artificial chromosome (BAC) clones flanking *USP6* (17p13) and *MYH9* (22q13.1) were obtained from Children's Hospital Oakland Research Institute (Oakland, CA). *USP6* BACs included RP11-167N20, RP11-910H9, RP11-211L24, RP11-106A7, RP11-198F11, RP11-115H24, RP11-124C16, RP11-457I18, RP11-1140D18, RP11-790C7, RP11-373N8, RP11-80K10 and RP11-960B9. *MYH9* BACs included RP11-

175G10, RP11-347K20, RP11-241E17, RP11-133I4, RP11-1056I22, RP11-643I13 and RP11-846O5. A D-FISH probe was constructed by labeling the 5′ end of *MYH9* in spectrum orange and the 3′ end of *USP6* in spectrum green. DNA isolation, nick translation and hybridization were performed as described previously.[19] Tissues were scored by two independent investigators and considered positive if ≥ 10% of 200 cells showed split signals. FISH images were captured using a Leica DM 6000 scope (Leica, Bannockbun, IL) with Cytovision software (Genetix, Boston, MA).

5′-RACE PCR

RACE-ready cDNA was generated using 1 μg of RNA from NF1 and NF2, using SMARTer RACE cDNA Amplification kit (Clonetech, Mountain View, CA) per manufacturer's instructions. 5′-RACE PCR was performed using touchdown PCR (five cycles of 94 °C 30 s, 72 °C 3 min; five cycles of 94 °C 30 s, 70 °C 30 s, 72 °C 3 min, and 25 cycles at 94 °C 30 s, 68 °C 30 s, 72 °C 3 min) with primers, universal primer (UPM; 5′-CTAATACGACTCACTATAGGGCAAGCAGTGGTATCAA CGCAGAGT-3′), *USP6* 3644 (5′-CCACATATGGCTTTTCAT GGACTCG-3′) and *USP6* 1747 (5′-CTTCCGCTCCTGTGC CTGCAAACTA-3′). Products were visualized on 3% gels and photographed using a DigiDoc-It imager (UVP, Upland, CA). DNA was extracted using Qiaquick gel extraction columns (Qiagen, Valencia, CA) per manufacturer instructions.

RT-PCR for MYH9-USP6

RT-PCR for *MYH9-USP6* fusion was performed on FFPE RNA. One microgram RNA was reverse transcribed using iScript Select cDNA Synthesis Kit (BioRad, Hercules, CA), using random primers per manufacturer instruction. PCR was performed using *USP6* primers (5′-TACGATCGGCCTCC TGGGATG-3′, 5′-CTTCCGCTCCTGTGCCTGCAAACTA-3′), *MYH9* primers (5′-ATCACCGCGGTTCCTG-3′, 5′-ACGGAA GGCTAAGCAAGGCTG-3′) and cycling conditions: 94 °C 2 min, 40 × (94 °C 30 s, 65 °C 30 s and 72 °C 30 s), with a final extension of 72 °C 10 min. Products were visualized on 3% gels and photographed using a DigiDoc-It imager (UVP). DNA was extracted using Qiaquick gel extraction columns (Qiagen) or ExoSap it (USB, Cleveland, OH) per manufacturer instruction.

Sequencing

Products were sequenced at the Mayo Clinic Sequencing Core, using the Applied Biosystems' BigDye XTerminator v1.1. kit chemistry for cycle sequencing and processed on a pair of ABI 3730/3730 × l DNA Analyzer capillary electrophoresis instruments (ABI, Foster City, CA).

Xenograft and Histological Analysis

MC3T3-E1 is a murine preosteoblastic cell line obtained from ATCC. *USP6* expression was placed under the control of a doxycycline (dox)-inducible promoter in MC3T3-E1 cells. *USP6*-transfected MC3T3-E1 cells (2.5E6 in 250 μl) were

Table 1 Clinical and molecular features of nodular fasciitis

ID	Sex/Age	Location	Size (cm)	USP6	MYH9	RT-PCR
1	M (44)	Palm	1.6	+	+	*MYH9-USP6*(I&II)
2	F (56)	Elbow	1.7	+	+	*MYH9-USP6*(I&II)
3	M (30)	Forehead		+	+	*MYH9-USP6*(I&II)
4	F (15)	Thorax		+	+	*MYH9-USP6*(I&II)
5	F (33)	Scapula		+	+	*MYH9-USP6*(I)
6	M (37)	Deltoid	4.8	+	+	*MYH9-USP6*(I)
7	F (53)	Forearm		+	+	*MYH9-USP6*(I)
8	F (20)	Ear	0.8	+	+	*MYH9-USP6*(I)
9	F (4)	Parietal		+	+	*MYH9-USP6*(I)
10	F (18)	Orbital	0.7	+	+	*MYH9-USP6*(I)
11	F (41)	Neck	1.7	+	+	*MYH9-USP6*(I)
12	M (13)	Shoulder	1.5	+	+	*MYH9-USP6*(I)
13	M (49)	Thigh		+	+	−
14	F (18)	Palm	2.5	+	+	−
15	M (36)	Shoulder	1.6	+	+	−
16	M (53)	Neck		+	+	−
17	M (9)	Back		+	+	ND
18	F (47)	Forearm	1.0	+	+	ND
19	M (50)	Eyelid		+	+	ND
20	M (29)	Pectoral		+	+	ND
21	M (36)	Shoulder		+	+	ND
22	F (54)	Heel		+	+	ND
23	F (9)	Hand		+	+	ND
24	F (20)	Ear	1.8	+	+	ND
25	M (29)	Forehead		+	+	ND
26	F (17)	Knee		+	+	ND
27	M (12)	Upper extremity		+	+	ND
28	M (59)	Axillary		+	+	ND
29	M (9)	Chest		+	+	ND
30	F (33)	Forearm		+	+	ND
31	F (33)	Forearm		+	+	ND
32	M (13)	Cheek		+	−	ND
33	F (52)	Neck		+	−	ND
34	F (55)	Back		+	−	ND
35	F (20)	Auricular	0.8	+	−	ND
36	F (21)	Forearm		+	−	ND
37	F (26)	Forearm	1.2	+	−	ND
38	F (48)	Submental	2.8	+	−	ND
39	M (31)	Thigh		+	−	ND
40	M (32)	Forearm		+	−	ND
41	F (48)	Forearm		+	−	ND
42	F (17)	Chin		+	−	ND
43	F (19)	Cervical mass		+	−	ND

Table 1 Continued

ID	Sex/Age	Location	Size (cm)	USP6	MYH9	RT-PCR
44	M (55)	Lumbar		+	−	ND
45	F (70)	Breast		−	−	ND
46	F (35)	Forearm		−	−	ND
47	F (16)	Back		−	−	ND
48	M (22)	Forearm		−	−	ND

Abbreviations: +, positive; −, negative for FISH and/or RT-PCR; M, male; F, female; ND, not done.

Age in years; cases 31–44 showed rearrangement of USP6 only (unknown partner gene).

injected subcutaneously into the rear flank. Nude male mice (4–8 weeks) were obtained from Jackson Laboratories and fed water containing 1 mg/ml dox (Research Products International, Mt Prospect, IL) supplemented with 5% sucrose for 1–2 weeks prior to xenografting. Following induction of the xenograft, dox was maintained in the drinking water and animals were monitored every 1–2 days for a period of 2–4 weeks.[20] All mouse procedures were conducted in accordance with guidelines set by IACUC at the University of Pennsylvania and Children's Hospital of Philadelphia. Tumors were paraffin-embedded, and histological analysis was performed by the Abramson Cancer Center Pathology Core of the University of Pennsylvania and Mayo Clinic. Histological sections (4 μm) were prepared and subjected to hematoxylin and eosin staining.

RESULTS
Clinical Findings
Clinical and molecular characteristics of NF ($n = 48$) are summarized in Table 1. Average age of NF patients was 33 years (range 4–70 years) with a 1:1.5 male to female ratio. Average lesion size was 1.8 cm (range: 0.7–4.8 cm), and the most common site of occurrence was the forearm ($n = 10$) (Table 1).

USP6 mRNA Expression Profiling
Screening of primary mesenchymal tumors and cell lines for *USP6* transcriptional upregulation revealed unusually high levels of *USP6* mRNA in NF, when compared with other tumors and normal tissues (Figure 1a). These unexpected findings led us to further explore possible mechanisms responsible for *USP6* mRNA transcriptional upregulation.

FISH for USP6, CDH11 and COL1A1
After excluding gene amplification by FISH and activating point mutations by direct sequencing (data not shown), we identified balanced rearrangement of *USP6* locus in 44 of 48
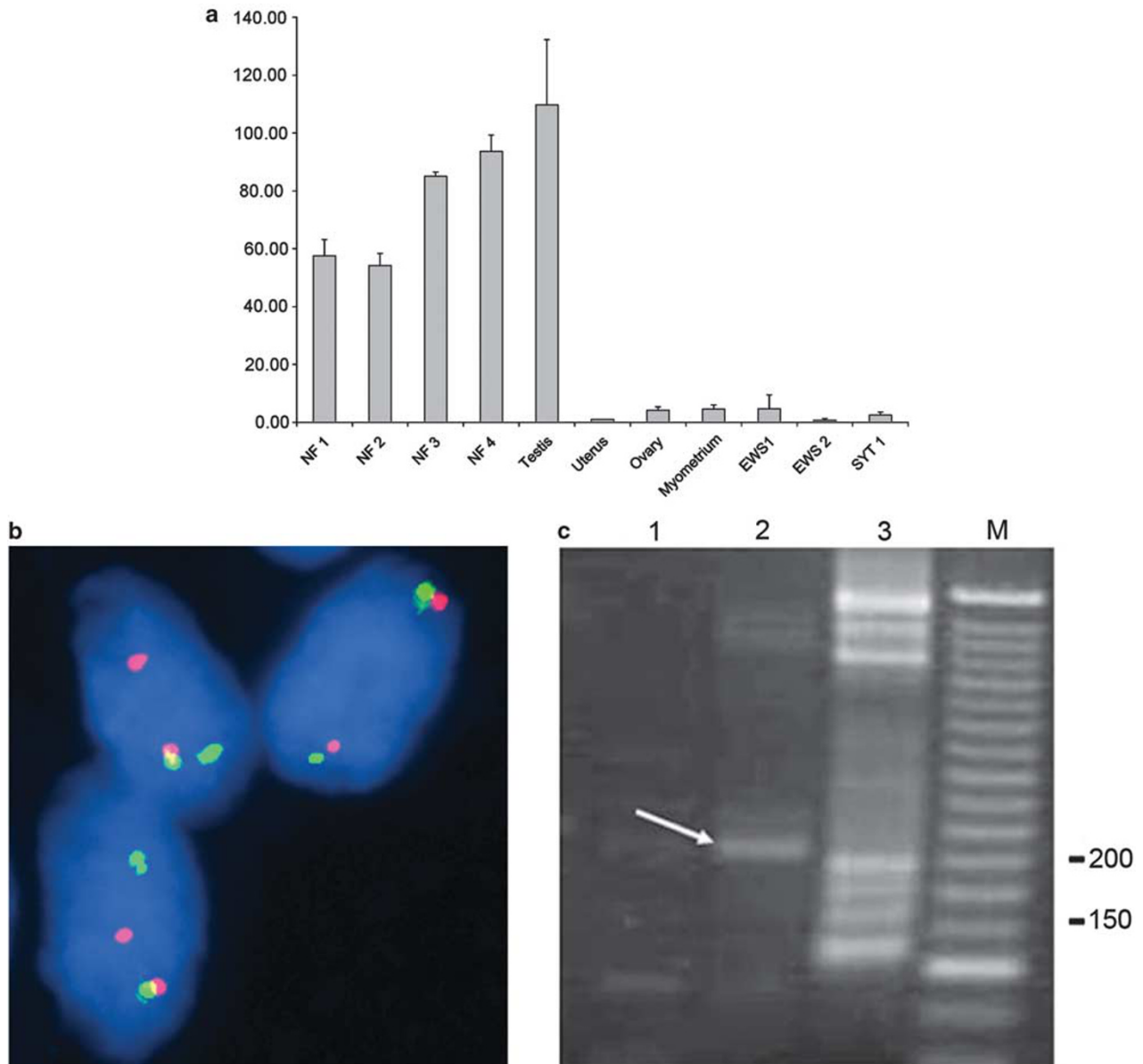
Figure 1 (**a**) qRT-PCR. All samples were normalized to uterus mRNA and relative mRNA expression is shown as a ratio along the *y* axis. Tissue and tumor samples are represented along the *x* axis (NF, nodular fasciitis, normal tissue (ovary, myometruim, uterus), testis mRNA (positive control); EWS, Ewing sarcoma; SYT, synovial sarcoma. (**b**) Fluorescent *in situ* hybridization (FISH) showing rearrangement of the *USP6* locus (separation of green and red signals). (**c**) 5′ RACE PCR. Lane 1, dH20; Lane 2, *MYH9-USP6* fusion (∼213 bp) using universal primer (UPM) + *USP6*_3644 (arrow); Lane 3, UPM + 746 *USP6* primer; M, 25-bp marker.

(92%) examples of human NF (Table 1 and Figure 1b). Considering that the pathogenesis of ABC is mediated by *USP6* oncogenic fusions with several partner genes with highly active promoters, most commonly *CDH11* and *COL1A1*,[12–17] we first excluded the involvement of these genes in NF by FISH and RT-PCR. No rearrangement of *CDH11* or *COL1A1* loci was found (data not shown).

5′-RACE PCR and Sequencing
5′ RACE on two examples of NF was then performed to identify a possible novel *USP6* fusion partner (Figure 1c); the fusion of *MYH9* exon 1 to *USP6* exons 1 and 2 was identified in both instances (Figure 2a).

RT-PCR and Sequencing
Specific RT-PCR confirmed the *MYH9-USP6* fusion; two splice variants recognized: *MYH9* non-coding exon 1 fused to *USP6* exon 1 (Type I 5′-GGGGCAGATCCAGGTTCAG-3′– 5′-GAAACTGGGCATCTCTGTGGC-3′; Genbank Accession no. 1385057) and *MYH9* non-coding exon 1 fused with *USP6* exon 2 (Type II 5′-GGGGCAGATCCAGGTTCAG-3′–5′-GAT GGACATGGTAGAGAATGC-3′; Genbank Accession no.
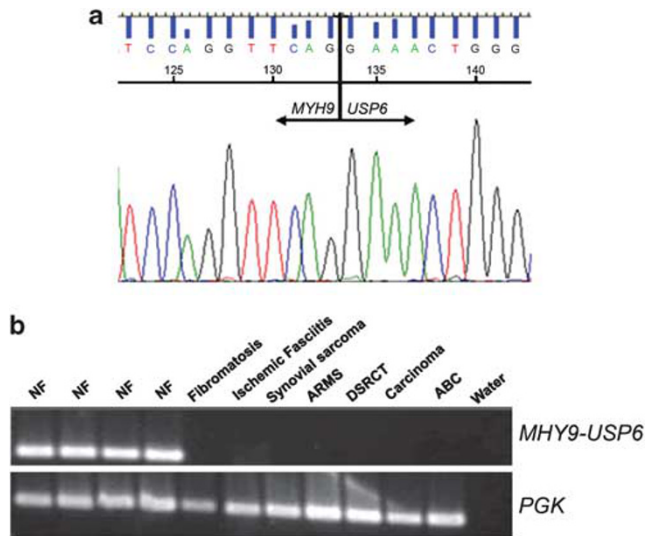
Figure 2 (a) Sequencing chromatogram of type I *MYH9-USP6* seen in nodular fasciitis (NF)-1 by both RACE and RT-PCR. (b) RT-PCR. Top panel: Lanes 1–4 demonstrate type I *MYH9-USP6* (~173 bp) fusion, which was only seen in human NF and not in other tumors studied (ARMS, alveolar rhabdomyosarcoma; DSRCT, desmoplastic small round cell tumor; ABC, aneurysmal bone cyst); lower panel, *PGK* (189 bp).

1394854). The *MYH9–USP6* fusion was found in 12 of 16 (75%) NF cases in which material was available; *MYH9–USP6* fusion transcripts were negative in all 43 controls tested (Figure 2b). Four examples of NF co-expressed the two fusion transcripts variants and the remaining eight expressed only the type I fusion (Table 1). No reciprocal fusion gene (*USP6–MYH9*) was identified.

FISH for MYH9

A balanced rearrangement of *MYH9* was found in 31/48 cases (65%) (Table 1, Figure 3a). To further confirm the fusion of *MYH9* to *USP6*, a dual FISH approach was taken and showed that the *MYH9* locus was juxtaposed to the *USP6* locus in all instances (Figure 3b). *MYH9* was only rearranged when *USP6* was also rearranged; *MYH9* was not rearranged in any of the 43 control tumors or other tissues tested (data not shown). Four examples of NF were negative for rearrangements of both *USP6* and *MYH9* loci (Table 1).

Xenograft Histological Analysis

We further sought to determine whether *USP6* over-expression was sufficient to elicit the formation of tumors that recapitulate human NF. *USP6* expression was placed under the control of a dox-inducible promoter MC3T3-E1 cells, and these cells were then injected subcutaneously in a similar location where NF often occurs. Xenografts yielded tumors clinically and histologically identical to human NF (Figures 3c, d, respectively). The lesions were characterized by a rapid proliferation of spindle cells associated with areas of hemorrhage and prominent mitotic activity (3–10/high

power fields). They become visible in 5–7 days, reached a maximum size (3–10 mm) within 2–3 weeks and then regressed (Figure 3c), mimicking closely the clinico-patho-logical features of human NF (Figure 3d).

DISCUSSION

NF is a self-limited, mass-forming subcutaneous myofibro-blastic proliferation of unknown etiology that predominantly affects younger individuals.[1,2] Interestingly, NF shows a peculiar clinical behavior characterized by spontaneous regression after a few weeks when not surgically excised; this peculiar clinical presentation has led to the historical view that NF is a reactive process of uncertain etiology.[1,2] Only rare examples of NF have been characterized at the cyto-genetic level, and no recurrent or consistent abnormality has been observed.[8–11] We first identified two cases of NF that expressed unexpected high levels of *USP6* mRNA. Sub-sequent studies showed 92% of NF contained rearrangements of the *USP6* locus and 65% of those formed the novel fusion *MYH9–USP6* (Table 1).

USP6 belongs to a large subfamily of de-ubiquitinating enzymes that act in diverse cellular processes such as intra-cellular trafficking, protein turnover, inflammatory signaling and cell transformation.[12,13] *USP6* is located on chromosome 17p13 and has very limited expression in normal cells (with predominant expression in testes).[12,13] *USP6* was first identi-fied as a possible oncogene when it exhibited transforming properties upon overexpression in NIH-3T3 cells.[12,13] Sub-sequently, our group identified *USP6* oncogenes in ABC, a locally recurrent mesenchymal neoplasm more commonly found in younger patients.[12–17] More recently, we reported the USP6-induced expression of matrix metalloproteases through activation of NF-κB, a transcription factor with a key role in inflammation and proliferation.[16]

MYH9 is located on chromosome 22q12.3-q13 and is a member of the non-muscle myosin class II family.[21–26] *MYH9* encodes for a protein involved in cytokinesis, cell motility, maintenance of cell shape, and more recently, found to have a direct role in actin network disassembly of crawling cells.[21–26] *MYH9* is found at relatively low levels in the body, except in fibroblasts, endothelial cells, macrophages, leukocytes and certain renal cells.[21–26] *MYH9* germline mutations have been reported in a number of human platelet disorders, and in 2003, Lamant *et al*[24] reported *MYH9* fused to *ALK* in an anaplastic large cell lymphoma. Another family member, *MYH11*, is fused to *CBFB* in acute myelogenous leukemia with eosinophilia.[25]

As previously mentioned, only a few NF has been char-acterized by standard cytogenetical analysis, but no specific abnormality has been found, except for an increased occur-rence of chromosome 15 rearrangements.[8–11] This observa-tion can be explained by the fact that both *MYH9* and *USP6* are located in light-stained terminal bands (22q12.3-q13 and 17p13, respectively), making the detection of this rearrangement quite challenging, using traditional
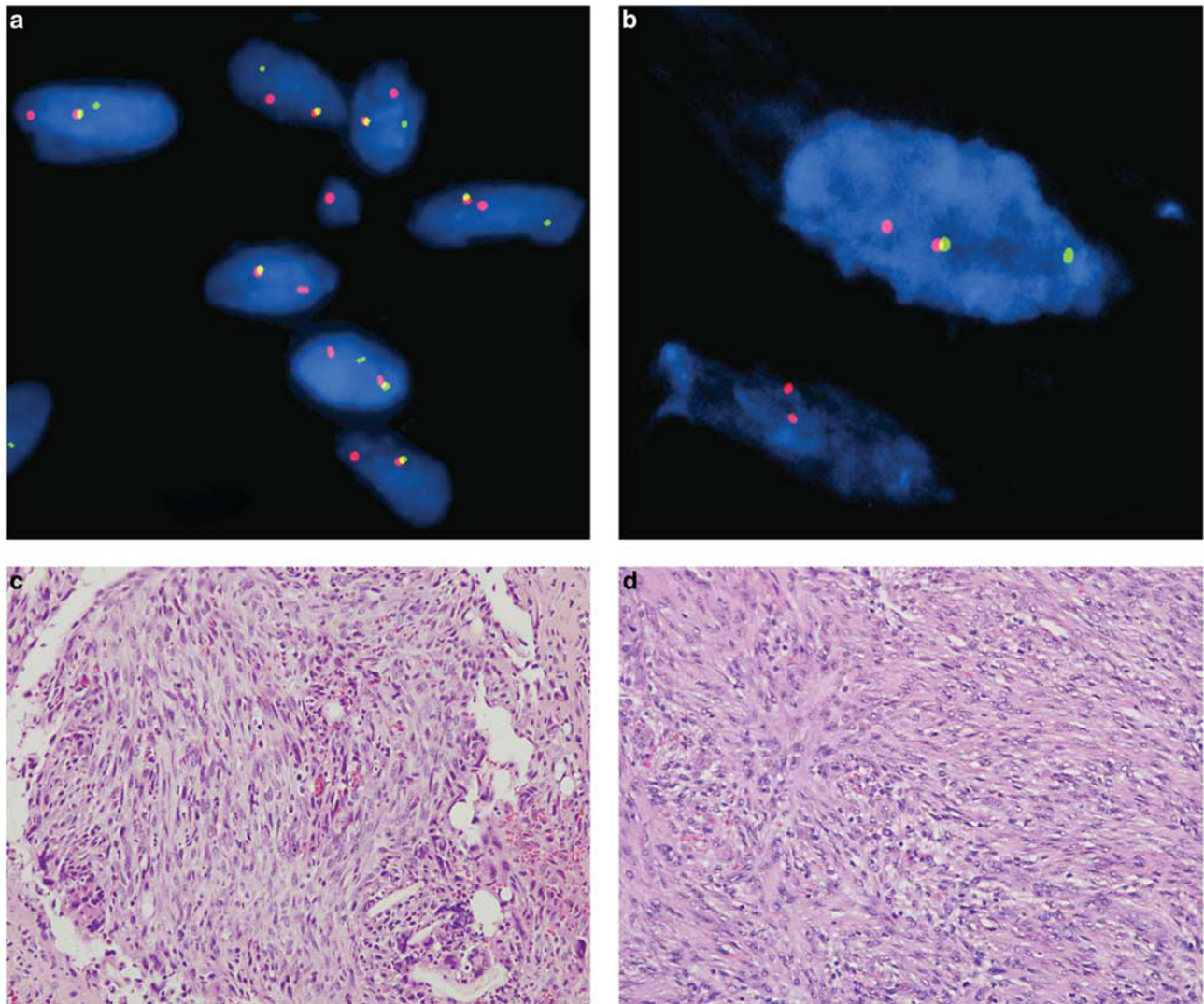
Figure 3 (**a**) Fluorescent *in situ* hybridization (FISH) showing rearrangement of the *MYH9* locus (separation of green and red signals). (**b**) D-FISH showing juxtaposition of *USP6* and *MYH9* loci (3′ *USP6* labeled in spectrum green and 5′ *MYH9* labeled in spectrum orange). (**c**) Mouse nodular fasciitis (NF)-like tumor induced by *USP6*-transfected pre-osteoblasts and (**d**) human NF (hematoxylin and eosin (HE) staining × 100).

cytogenetical analysis.[27] A similar situation can be exemplified with *ETV6 (TEL)–NTRK3* fusion in infantile fibrosarcoma, which went undetected for years using traditional cytogenetical analysis, because both genes are located at the end of chromosomes 12 and 15, respectively.[28,29]

Interestingly, ABC and NF have overlapping histological features that have not been previously emphasized. Both are characterized by a proliferation of bland spindle cells intermixed with inflammatory cells.[1,2,30] Although hemorrhagic cysts are typical of ABC, extravasated erythrocytes and microcystic formation are typically present in NF.[1,2,30] These similarities suggest that these histological manifestations may have a common pathogenic denominator mediated by *USP6* transcriptional upregulation.

Our findings also suggest that, although *USP6* transcriptional upregulation may be the driving force behind the high proliferative activity and growth of NF, the consistent involutional nature of the lesion indicates that additional genetical or stromal factors are required for maintaining its long-term survival and viability. Moreover, NF appears to be the first example of a self-limited, tumor-like lesion, characterized by a recurrent, somatic gene fusion event. This finding challenges the traditional concept that acquired nonrandom fusion gene abnormalities are the sole domain of sustained, autonomous neoplastic proliferations. In this regard, the hematopoietic system is most informative for comparative purposes. Although several examples of aberrant lymphoma-associated gene fusion events are described in B-lymphocyte populations with increasing age, these occurrences are incidental and do not manifest as self-limited, tumor-like expansions.[31] Future studies are necessary to better understand the mechanism by which the oncogenic

activation of *USP6* generates the unique clinical behavior of NF.

Furthermore, the identification of a sensitive and specific abnormality in NF also holds the potential to be used diagnostically.

In conclusion, our study uncovers the etiology of an entity whose pathogenesis has otherwise long remained a mystery. The mechanism seems to involve *USP6* transcriptional up-regulation due to its fusion with a strong ectopic promoter (*MYH9*). The identification of a sensitive and specific abnormality in NF holds the potential to provide a novel diagnostic avenue for these lesions. More importantly, NF seems to be the first example of a self-limited human lesion, characterized by a recurrent somatic gene fusion event.

DISCLOSURE/CONFLICT OF INTEREST
The authors declare no conflicts of interest.

1. Fletcher CDM, Unni KK, Mertens F. World Health Organization classification of tumours. Pathology and Genetics of Tumours of Soft Tissue and Bone. Lyon: France, 2005.
2. Kumar V, Abbus AK, Fausto N, *et al*. Robbins & Cotran Pathologic Basis of Disease. In Elsevier Saunders: Philadelphia, PA, 2004; 1318.
3. Velagaleti GV, Tapper JK, Panova NE, *et al*. Cytogenetic findings in a case of nodular fasciitis of subclavicular region. Cancer Genet Cytogenet 2003;141:160–163.
4. Tomita S, Thompson K, Carver T, *et al*. Nodular fasciitis: a sarcomatous impersonator. J Pediatr Surg 2009;44:e17–e19.
5. Wagner LM, Gelfand MJ, Ryckman FC, *et al*. A welcome surprise: nodular fasciitis presenting as a soft tissue sarcoma. J Pediatr Hematol Oncol 2010.
6. Silvanto AM, Melly L, Hannan SA, *et al*. FNAC of nodular fasciitis mimicking a pleomorphic adenoma: another diagnostic pitfall. Cytopathology 2010;21:276–277.
7. Konwaler B, Keasbey L, Kaplan L. Subcutaneous pseudosarcomatous fibromatosis (fasciitis). Am J Clin Pathol 1955;25:241–252.
8. Sawyer JR, Sammartino G, Baker GF, *et al*. Clonal chromosome aberrations in a case of nodular fasciitis. Cancer Genet Cytogenet 1994;76:154–156.
9. Weibolt VM, Buresh CJ, Roberts CA, *et al*. Involvement of 3q21 in nodular fasciitis. Cancer Genet Cytogenet 1998;106:177–179.
10. Donner LR, Silva T, Dobin SM. Clonal rearrangement of 15p11.2, 16p11.2, and 16p13.3 in a case of nodular fasciitis: additional evidence favoring nodular fasciitis as a benign neoplasm and not a reactive tumefaction. Cancer Genet Cytogenet 2002;139:138–140.
11. Birdsall SH, Shipley JM, Summersgill BM, *et al*. Cytogenetic findings in a case of nodular fasciitis of the breast. Cancer Genet Cytogenet 1995;81:166–168.
12. Oliveira AM, Perez-Atayde AR, Inwards CY, *et al*. USP6 and CDH11 oncogenes identify the neoplastic cell in primary aneurysmal bone cysts and are absent in so-called secondary aneurysmal bone cysts. Am J Pathol 2004;165:1773–1780.
13. Oliveira AM, Perez-Atayde AR, Dal Cin P, *et al*. Aneurysmal bone cyst variant translocations upregulate USP6 transcription by promoter swapping with the ZNF9, COL1A1, TRAP150, and OMD genes. Oncogene 2005;24:3419–3426.
14. Oliveira AM, Chou MM, Perez-Atayde AR, *et al*. Aneurysmal bone cyst: a neoplasm driven by upregulation of the USP6 oncogene. J Clin Oncol 2006;24:e1.
15. Oliveira AM, Hsi BL, Weremowicz S, *et al*. USP6 (Tre2) fusion oncogenes in aneurysmal bone cyst. Cancer Res 2004;64:1920–1923.
16. Ye Y, Pringle LM, Lau AW, *et al*. TRE17/USP6 oncogene translocated in aneurysmal bone cyst induces matrix metalloproteinase production via activation of NF-kappaB. Oncogene 2010;29:3619–3629.
17. Lau AW, Pringle LM, Quick L, *et al*. Tre17/ubiquitin-specific protease 6 (USP6) oncogene translocated in aneurysmal bone cyst blocks osteoblastic maturation via an autocrine mechanism involving bone morphogenetic protein dysregulation. J Biol Chem 2010;285:37111–37120.
18. Qian X, Jin L, Shearer BM, *et al*. Molecular diagnosis of Ewing's sarcoma/primitive neuroectodermal tumor in formalin-fixed paraffin-embedded tissues by RT-PCR and fluorescence *in situ* hybridization. Diagn Mol Pathol 2005;14:23–28.
19. Erickson-Johnson MR, Seys AR, Roth CW, *et al*. Carboxypeptidase M: a biomarker for the discrimination of well-differentiated liposarcoma from lipoma. Mod Pathol 2009;12:1541–1547.
20. Welman A, Barraclough J, Dive C. Generation of cells expressing improved doxycycline-regulated reverse transcriptional transactivator rtTA2S-M2. Nat Protoc 2006;1:803–811.
21. D'Apolito M, Guarnieri V, Boncristiano M, *et al*. Cloning of the murine non-muscle myosin heavy chain IIA gene ortholog of human MYH9 responsible for May-Hegglin, Sebastian, Fechtner, and Epstein syndromes. Gene 2005;286:215–222.
22. Wilson CA, Tsuchida MA, Allen GM, *et al*. Myosin II contributes to cell-scale actin network treadmilling through network disassembly. Nature 2010;465:373–377.
23. Hu A, Wang F, Sellers JR. Mutations in human nonmuscle myosin IIA found in patients with May-Hegglin anomaly and Fechtner syndrome result in impaired enzymatic function. J Biol Chem 2002;277:46512–46517.
24. Lamant L, Gascoyne RD, Duplantier M, *et al*. Non-muscle myosin heavy chain (MYH9): a new partner fused to ALK in anaplastic large cell lymphoma. Genes Chromosomes Cancer 2003;37:427–432.
25. Landrette SF, Kuo YH, Hensen K, *et al*. Plag1 and Plag2 are oncogenes that induce acute myeloid leukemia in cooperation with Cbfb-MHY11. Blood 2005;105:2900–2907.
26. Heath KE, Campos-Barros A, Toren A, *et al*. Nonmuscle myosin heavy chain IIA mutations define a spectrum of autosomal dominant macrothrombocytopenias: May-Hegglin anomaly and Fechtner, Sebastian, Epstein, and Alport-like syndromes. Am J Hum Genet 2001;69:1033–1045.
27. Shaffer LG, Tommerup N (eds). An International System for Human Cytogenetic Nomenclature (ISCN). S Karger, Basel, 2005.
28. Knezevich SR, McFadden DE, Tao W, *et al*. A novel ETV6-NTKR3 gene fusion in congenital fibrosarcoma. Nat Genet 1998;18:184–187.
29. Rubin BP, Chen CJ, Morgan TW, *et al*. Congenital mesoblastic nephroma t(12;15) is associated with ETV6-NTKR3 gene fusion: cytogenetic and molecular relationship to congenital (infantile) fibrosarcoma. Am J Pathol 1998;153:1451–1458.
30. Allen PW. Nodular fasciitis. Pathology 1972;4:9–26.
31. Brassesco M. Leukemia/lymphoma-associated gene fusions in normal individuals. Genet Mol Res 2008;7:782–790.